

# Large Clusters of Metal Ions: The Transition from Molecular to Bulk Magnets

Dante Gatteschi,\* Andrea Caneschi, Luca Pardi, Roberta Sessoli

Clusters of metal ions are a class of compounds actively investigated for their magnetic properties, which should gradually change from those of simple paramagnets to those of bulk magnets. However, their interest lies in a number of different disciplines: chemistry, which seeks new synthetic strategies to make larger and larger clusters in a controlled manner; physics, which can test the validity of quantum mechanical approaches at the nanometer scale; and biology, which can use them as models of biomineralization of magnetic particles.

The prefix nano- seems to be the theme of the last decade of this century, allowing us new perspectives in many different fields. Nanoscale electronics is coming of age, but many other disciplines share the interest for the mesoscopic regime of matter. Among them, chemistry is becoming more and more involved in the synthesis of large assemblies of molecules (supramolecular chemistry) and of new large molecules. Examples of the latter class are provided by large metal ion clusters, of which an aesthetically rewarding case is the  $[\text{Mn}(\text{hfac})_2\text{NITPh}]_6$  cluster (1) (Fig. 1) (hfac, hexafluoroacetyl acetate; NITPh, 2-phenyl-4,4,5,5-tetramethyl-4,5-dihydro-1H-imidazolyl-1-oxy-3-oxide). The manganese(II) ions, with  $S = \frac{1}{2}$ , are connected by organic radicals NITPh,  $S = \frac{1}{2}$ . The two types of spins are strongly antiferromagnetically coupled (exchange coupling constant  $J > 250$  K) in such a way that the ground state can be described as having all the manganese spins up and the radical spins down, to give a ground state with  $S = 12$ . Ground states with such large spins are rare, and a material like  $[\text{Mn}(\text{hfac})_2\text{NITPh}]_6$  can be used as a first step toward the investigation of the magnetic properties of nanoscale molecular materials.

We report here on the molecular approaches to nanoscale magnetic particles. One of the purposes of such investigations is finding the link between simple paramagnetic and bulk magnetic behavior. Molecular chemistry can give strategies for making large molecules containing many magnetic centers, be they metallic ions or organic radicals, ideally adding one center at a time. The magnetic properties of the molecule may then be measured, and when they can no longer be interpreted within the simple schemes of paramagnetism, more complex schemes of cooperative magnetism can be explicitly introduced.

The intermediate region of nanoscale magnetic particles is of large interest in solid-state

physics (2–7) because it can be expected that classical and quantum behavior coexist (8, 9) (quantum tunneling of the magnetization in large-spin clusters, for instance). Experiments in this type of particles are expected to provide confirmation of the quantum theory itself.

Molecular approaches are not the only possible routes to nanoscale magnetic particles. Indeed, important results have been recently obtained by the preparation of nanoscale metal clusters (10, 11) with sophisticated techniques, for instance, with the use of a modified scanning microscope, to locally decompose iron pentacarbonyl molecules,  $\text{Fe}(\text{CO})_5$ . Many methods are also available for rapid precipitation of ionic compounds, such as spinels. However, these methods do not give monodispersed particles, and it is not possible to control their solubility in organic solvents, that is, they do not have the properties of molecular aggregates.

Large metal ion clusters are also important for their relevance to biological systems (12, 13). For instance, compounds that contain large numbers of iron and manganese ions may behave similarly to the metal ion clusters present in biological systems such as photosystem II, the center responsible for photosynthesis in bacteria, and ferritin, the iron-storage protein.

A particularly illuminating example of this is shown (14) in Fig. 2. The molecule contains 17 iron(III) ions (which are connected by various bridges), O, OH, and RO. The peripheral iron ions are coordinated by organic ligands,  $\text{N}(\text{CH}_2\text{COOH})_2(\text{CH}_2\text{CH}_2\text{OH})$  ( $\text{H}_3\text{heidi}$  for short), which stabilize the molecule. The role of the ligands is clearly shown in Fig. 2B: The inorganic core has almost completely disappeared, secluded from contact with the external environment by the ligands that provide a hydrophobic protection. Thus, it has similarities with ferritin, in which an iron oxo or hydroxo core of  $\sim 70$  Å is contained in a proteic sphere (15). These clusters can be considered as an intermediate in the growth of iron oxides and hydroxides. Other iron oxo clusters have been suggested to be more appropriate models for ferritin (16). The cluster of Fig. 2 has a central core of seven iron(III)

ions, which corresponds to a small part of the lattice of goethite,  $\text{FeO}(\text{OH})$ , which is the final hydrolysis product of iron salts.

We report recent advances in the understanding of the magnetic properties of large molecular aggregates, which have well-defined molecular weights, which can be crystallized, and whose x-ray crystal structure can be determined. The interpretation of the magnetic properties of these materials poses several problems because they are too complex to be treated as simple paramagnets, but at the same time, their lack of translational symmetry does not allow many of the simplifications used for infinite arrays of spins.

We consider three classes of materials—polyoxovanadates(IV), polyiron, and polymanganese oxo clusters—which we feel are the most relevant examples available, demonstrating the state of the art in this field. There are other classes of materials that are molecular and might also be included in the review, like the poly iron thio derivatives made by Holm and co-workers (17) in a successful effort to mimic the properties of iron sulfur proteins, but for reasons of space, we will not be able to discuss these.

## Polyoxovanadates and Magnetic Multilayers

Polyoxometallates, which spontaneously form for certain ions like vanadium(V), molybdenum(VI), and tungsten(VI), are well known (18). These compounds have been investigated for many different properties ranging from catalysis to possible use

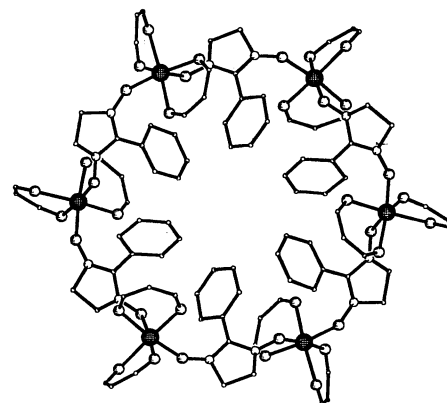


**Fig. 1.** View of the  $[\text{Mn}(\text{hfac})_2\text{NITPh}]_6$  cluster, where, for clarity, the methyl and trifluoromethyl groups are omitted. The manganese atoms are represented by cross-hatched disks, and the oxygen, nitrogen, and carbon atoms are shown as empty circles of decreasing size.

D. Gatteschi, A. Caneschi, and R. Sessoli are with the Department of Chemistry, University of Florence, Florence, Italy. L. Pardi is with the Laboratoire L. Brillouin, CEN Saclay, 91191 Gif-sur-Yvette, France.

as antiretroviral drugs (19). Recently, much interest focused on the magnetic properties of these materials and many compounds comprising large numbers of coupled metal ions have been reported. For instance, classes of polyoxometallates comprising magnetic ions like vanadium(IV) and molybdenum(V), both with one unpaired electron, have been reported by Müller and co-workers (20–23).

The polyoxovanadate containing the largest number of magnetic ions for which a detailed interpretation of the magnetic properties is available is  $[V_{15}As_6O_{42}(H_2O)]^-$ , referred to here as  $V_{15}$  (24) (Fig. 3). All of the vanadium ions have  $S = 1/2$  and are antiferromagnetically coupled to give a ground state with  $S = 1/2$ . The interesting feature of the structure and of the magnetic properties (25) of this compound is that the metal ions are arranged in three planes, of six, three, and six ions, respectively. These three planes behave differently from each other: The strong couplings in the hexagonal layers quench their magnetization at relatively high temperatures, and the three spins in the middle layer remain largely uncoupled down to very low temperatures. In fact, the spins in the middle layer are antiferromagnetically coupled among themselves and with the other spins of the other two layers, but their triangular arrangement gives rise to degeneracy in the low-lying levels. When three spins are arranged on an equilateral triangle and are antiferromagnetically coupled,

that is, when they tend to be antiparallel to each other in pairs, one spin cannot be antiparallel to the other two at the same time. With the adoption of a term from psychology, the spin is then said to be frustrated (26) because it is under the influence of two contrasting stimuli to which it cannot respond adequately at the same time.

The magnetic properties of  $V_{15}$  have been satisfactorily analyzed, and the spin levels have been calculated with a model of Heisenberg exchange. In principle, the number of states to be included in the calculation for a cluster of  $N$  identical spins  $S$  is given by  $(2S+1)^N$ , giving in the present case 32,768 states. The dimensions of the matrices can be reduced by taking advantage of the total spin symmetry, that is, of the fact that nonzero matrix elements can be found only between states with the same value of the total spin  $S = \sum S_i$ . The states must therefore be classified according to  $S$ , which in this case, ranges from  $15/2$  to  $1/2$ . There are 16 matrices to be calculated, whose dimensions range from 1 to 2002. In order to reduce the time needed to calculate the matrices, use is made of irreducible tensor operators, which allow an elegant exploitation of the symmetry. A computer program, CLUMAG (27), was used, which can perform the calculation with arbitrary values of  $N$  and  $S_i$  and can use point group symmetry to reduce the dimensions of the matrices.

A cluster of 15 ions each with  $S = 1/2$ , although large, is still far from the limits of bulk behavior, presumably because of the quantum nature of the  $S = 1/2$  spins. The required number of centers to be assembled decreases if we use building blocks possessing individual spins that are closer to the classical limit, for example,  $S = 5/2$ .

### Iron Clusters and Metamagnetism

Iron clusters provide a much larger variety of spin values, and indeed, very high ground

spin states have been observed for these materials. An example is a cluster of eight iron(III) ions (28) (Fig. 4). There are four ions in the middle of the molecule in an arrangement that is well known in tetranuclear clusters, the butterfly arrangement. The motif can be considered as the first step toward the formation of a triangular planar lattice. As such, the spins on the metal ions are highly frustrated in the case of antiferromagnetic coupling. This means that it will be impossible to predict the preferred spin alignment in this cluster with hand-waving arguments associated with dispositions of spins up or down. The four central iron(III) ions are connected to the four peripheral iron(III) ions by hydroxo bridges. At the exterior of the molecule, the organic ligands provide the required hydrophobicity, which prevents the growth of the iron hydroxide.

The central motif becomes more complex in the structure of two clusters (14) containing 19 and 17 iron ions. The structure of  $Fe_{17}$  was shown in Fig. 2. That of  $Fe_{19}$  is very similar, with two additional iron ions in the periphery of the molecule on opposite sides. The central group of seven iron ions is identical in the two molecules, confirming their validity as models of iron biomineralization. The two molecules crystallize together on the same lattice.

The last example has an essentially one-dimensional structure, at least from the magnetic point of view (Fig. 5). It comprises 10 iron(III) ions in a ring,  $Fe_{10}$ , which has been called a ferric wheel (29).

The magnetic properties of  $Fe_8$  and of  $Fe_{17}+Fe_{19}$  are rather similar to each other (30, 31) (Fig. 6). A qualitative analysis of the susceptibility  $\chi$  and temperature  $T$  data shows that in these compounds there are antiferromagnetic interactions: The room-temperature values (2.5 and 3 emu mol<sup>-1</sup> K) are much lower than expected for uncou-

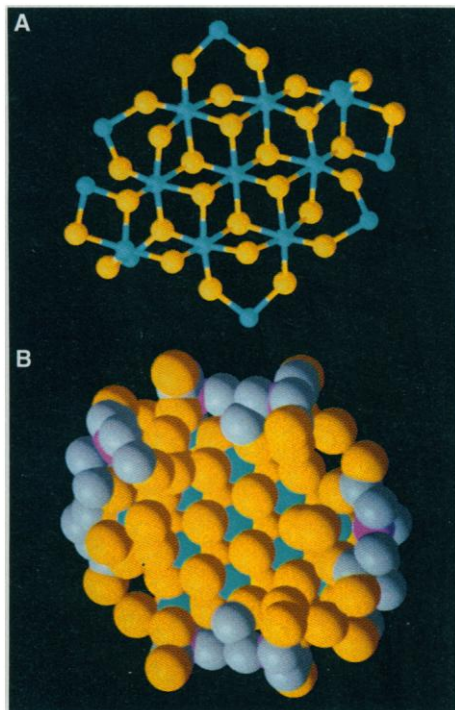


**Fig. 2.** Schematic view of the  $Fe_{17}$  cluster where (A) only the metal atoms, in light blue, and bridging oxygen atoms, in yellow, are shown and (B) spheres proportional to the van der Waals radii are drawn in light blue for iron, yellow for oxygen, purple for nitrogen, and gray for carbon atoms.

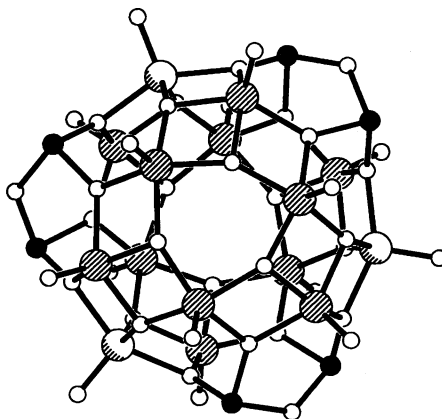


**Fig. 3.** View of the  $V_{15}$  cluster. A disordered water molecule is trapped in the central cavity of the cluster but not shown. The filled circles represent the arsenic atoms, and the small empty circles, the oxygen atoms. The large circles are vanadium atoms, and those defining the six membered rings are hatched.

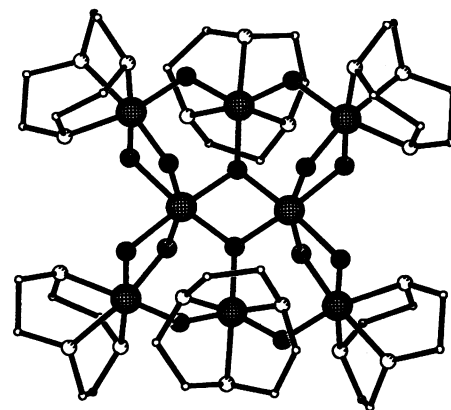


**Fig. 4.** Structure of the  $Fe_8$  cluster. The cross-hatched circles are the metal atoms, the hatched circles are the oxygen atoms, and the empty circles represent, in order of decreasing size, nitrogen and carbon atoms.

pled spins ( $4.375 \text{ emu mol}^{-1} \text{ K}$ ). As temperature decreases,  $\chi T$  increases, showing that the individual moments do not compensate. These molecules therefore are examples of ferrimagnetic materials. The low temperature value of  $\chi T$  and of the magnetization of  $\text{Fe}_8$  indicate a ground-state spin of  $S = 9$  or 10.

The  $\text{Fe}_{17}$  and  $\text{Fe}_{19}$  clusters do not correspond to two different compounds but crystallize together in the same cell. Therefore, the magnetic data are more difficult to interpret, even at the qualitative level. Magnetization data at 1.85 K show a rapid saturation to a limit value of  $\sim 65 \mu_B$  per  $\text{Fe}_{17} + \text{Fe}_{19}$  unit, where  $\mu_B$  is the Bohr magneton. If the observed magnetization is equally shared between the two clusters, it becomes apparent that the spin of the ground state of the cluster cannot be smaller than  $3\frac{1}{2}$ , which is the largest moment so far reported for an individual molecule.

A quantitative interpretation of the magnetic properties of these compounds has been possible only for  $\text{Fe}_8$ , and this at the cost of some effort (30), the total number of states being 1,679,616. Exploiting symmetry allows the reduction of the problem to that of calculating 81 matrices, ranging in dimensions from 1 to 4170. In this way, the problem becomes tractable, even if no best-fit procedure can be attempted. However, the ground state can be estimated to be either  $S = 9$  or 10 as a result of competing antiferromagnetic interactions, in accord with the qualitative description given above.

A similar analysis proved (31) to be impossible for the  $\text{Fe}_{17}$  and  $\text{Fe}_{19}$  clusters. Even with use of all of the possible symmetries, the dimensions of the matrices remain much too large to be tackled with the standard approach. In this field, theoretical de-

velopments are strongly needed so that we can interpret the thermodynamic properties of the new materials. Theoreticians have a large number of molecules on which to test their theories.

More elegant and better understood results (32) were obtained from the analysis of the magnetic properties of  $\text{Fe}_{10}$ . This is an ideal compound long used to extrapolate the thermodynamic properties of infinite chains. The magnetic susceptibility of  $\text{Fe}_{10}$  goes through a maximum at  $\sim 60 \text{ K}$ , a clear indication of antiferromagnetic interactions within the ring. Unfortunately, even in this case it was impossible to make a quantitative calculation because the maximum number of coupled  $S = \frac{1}{2}$  spins that we can include in our computer program is eight. However, calculations on rings of four, six, and eight members showed that reduced susceptibility versus reduced temperature rapidly converge, so that the calculated curves for  $N = 8$  spins can be extrapolated without much error to  $N = 10$ . Indeed, the agreement between experimental and calculated  $\chi$  is very good for  $J = 13.5 \text{ K}$ . Similar results were obtained with a model with classical spins instead of quantum spins. The approximation in this case should be reasonable because the individual spins are fairly large ( $S_i = \frac{5}{2}$ ).

The magnetization data of  $\text{Fe}_{10}$  at very low temperature provided additional information on the energies of the lowest excited levels. At low field, the magnetization is zero, in agreement with an  $S = 0$  ground state, but above 4 T, it rapidly increases, reaching the value of  $2 \mu_B$ , appropriate for an  $S = 1$  spin (Fig. 7). This indicates that the external magnetic field stabilizes a low-lying  $S = 1$  state, which becomes the ground state.

As the field is increased, other similar steps are observed, with plateaus at 4, 6, and  $8 \mu_B$ , indicating that states with total spins  $S = 2, 3, 4, \dots$  successively become the ground state (Fig. 7). The experiments with pulsed fields that measure  $dM/dB$  confirm this view, showing peaks (Fig.

8) with maxima corresponding to the inflection points of the static magnetization. In the highest field that could be reached with the experimental apparatus, 42 T, the ground state becomes  $S = 9$ .

The  $\text{Fe}_{10}$  ring is a paramagnet, and its ground state is nonmagnetic rather than antiferromagnetic. However, the observed behavior of its magnetization is representative of the metamagnetic behavior observed in bulk antiferromagnets. In a metamagnet, some spins in a lattice are reversed by an applied field, which provides enough energy to reverse some spins from their preferred orientation determined by the magnetic interactions with the other spins.

The field separations between neighboring peaks, corresponding to crossover from one spin state to the other, are all practically identical to each other (Fig. 8). This is a clear indication of the difference in the energies of the levels with different  $S$  in zero field. The lowest level of each multiplet can be considered to decrease its energy linearly in the applied magnetic field with a slope proportional to  $-S$  (Fig. 7). The fact that the crossovers occur at regular intervals implies that the energy levels follow a Lande interval rule

$$E(S) = (P/2) S(S + 1) \quad (1)$$

The constant  $P$  is experimentally determined to be 4.27 K.

The lowest energy levels for every  $S$  value can be calculated within an approximate model, which provides a relation between  $P$  and the exchange coupling constant  $J$  between nearest neighbors

$$J = NP/2 \quad (2)$$

This relation shows that the separations between the low-lying levels go to zero when  $N$ , the number of spins in the ring, tends to infinity.

Although large-spin ground states have been observed for some of these com-

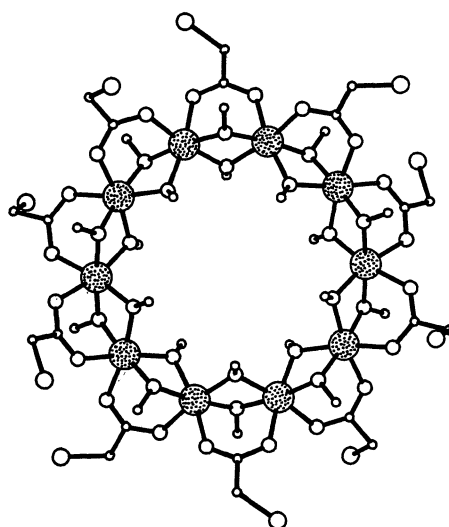


Fig. 5. View of the ring structure of the  $\text{Fe}_{10}$  cluster, where the dotted circles represent the iron atoms and the empty circles are, in order of decreasing size, chlorine, oxygen, and carbon.

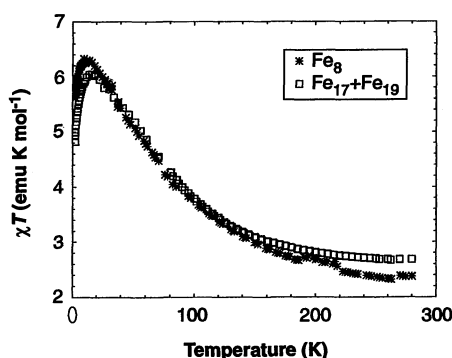


Fig. 6. Temperature dependence of the product of the magnetic susceptibility and temperature of  $\text{Fe}_8$  and  $\text{Fe}_{17+19}$  clusters. The values are given per iron atom.

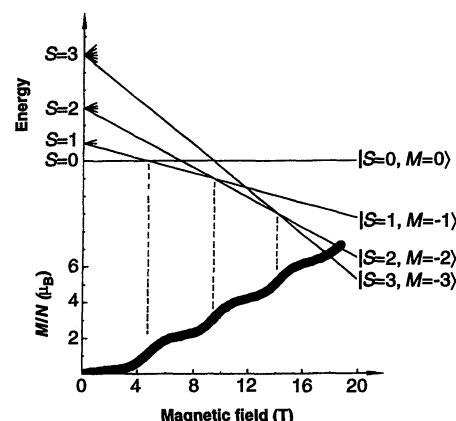


Fig. 7. (Top) The energy of the spin levels and the crossovers induced by the increasing field. (Bottom) The static magnetization of  $\text{Fe}_{10}$  measured at 0.65 K.

pounds, magnetic susceptibility measurements did not reveal any hint of bulk behavior. In principle, it might be expected that at some stage, superparamagnetic behavior should be observed. A superparamagnet is a single-domain magnetically ordered material in which the barrier to the reorientation of the magnetization is comparable to thermal energy (33). As a consequence, the magnetization flips freely and its time average is zero, as in a paramagnet. In an external field, it behaves like a paramagnet, with  $S = \infty$ . When the temperature is sufficiently reduced, the barrier is restored and the magnetization becomes blocked; that is, below a blocking temperature  $T_b$ , the superparamagnet reverts to usual bulk (ferro-, ferri-, or antiferromagnetic) behavior. In fact, the frequency of the reorientation of the magnetization is given by

$$\nu = \nu_0 \exp(-E_A/k_B T) \quad (3)$$

where  $\nu_0$  is a constant characteristic of the material,  $E_A$  is the magnetic anisotropy energy of the particle, and  $k_B$  is Boltzmann's constant. For a particle with uniaxial anisotropy,  $E_A$  is usually written as

$$E_A = KV \quad (4)$$

where  $K$  is the anisotropy constant per unit volume and  $V$  is the volume of the particle.

The blocking temperature depends on the time scale,  $\tau_{\text{exp}}$ , of the investigating technique. For instance, for magnetic susceptibility experiments,  $\tau_{\text{exp}}$  is of the order of  $10^{-2}$  s, whereas for Mössbauer spectroscopy,  $\tau_{\text{exp}} = 10^{-8}$  s. Therefore, the latter technique monitors higher blocking temperatures than the first. The Mössbauer spectrum for a fast-relaxing iron paramagnet yields a doublet; however, when the reorientation of the magnetization becomes longer than  $\tau_{\text{exp}}$ , a sextet spectrum is observed (34).

Papaefthymiou and co-workers analyzed

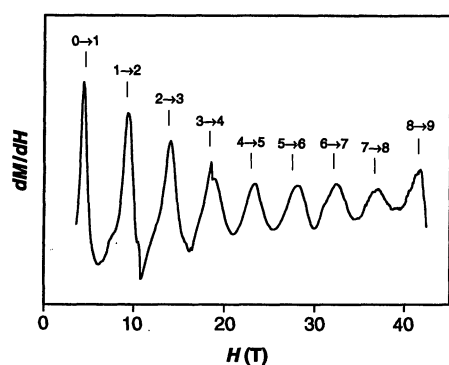


**Fig. 8.** Derivative of the magnetization versus applied magnetic field for the  $\text{Fe}_0$  cluster, observed in a pulsed experiment at 0.65 K in a field up to 42 T. The maxima show the crossovers to states of higher spin multiplicity, and the vertical lines represent the fields calculated for each spin crossover with the use of a  $P$  value of  $4.27 \text{ cm}^{-1}$ , as described in the text.

the spectra of several polyiron oxo and thio clusters (16, 35, 36) in the temperature range of 4 to 300 K and, in some cases, found a sextet spectrum in the absence of an applied field. From comparison of the Mössbauer spectra recorded with and without an external magnetic field, she concluded that some of them behave as superparamagnets and that, because the clusters showing this behavior have a pseudo three-dimensional structure, it must be expected that bulk behavior shows up at an earlier stage in pseudo three-dimensional than it does in pseudo one- and two-dimensional particles. Although this is a rational statement, more experimental work, by a technique that uses a different frequency window or characterizes the magnetic anisotropy, is needed to confirm it. Indeed, in a manganese cluster, which shows much longer relaxation times of the magnetization, the structure is more two- than three-dimensional.

### Manganese Clusters and Molecular Magnetic Bistability

The electron paramagnetic resonance (EPR) spectra of  $[\text{Mn}(\text{hfac})_2\text{NITPh}]_6$  (1) (structure in Fig. 1) show some interesting features. At high temperature, their linewidths follow an angular dependence similar to those observed (37) for both one- and two-dimensional magnetic materials, that is, for materials in which an infinite number of interacting spins are arranged in chains or in layers, respectively. Therefore, it might seem that an incipient bulk behavior is starting to show up. However, the analysis of the line shapes raises some doubts on this issue. In fact, for infinite lattices, the line shape is intermediate between a Gaussian and a Lorentzian. The one-dimensional line shape is closer to the former limit, and the observed line shape in the cluster is Gaussian, suggesting that the line is

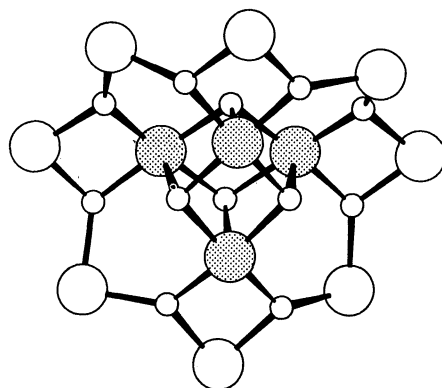


**Fig. 9.** Schematic view of the core of a  $[\text{Mn}_{12}\text{O}_{12}(\text{carboxylato})_{16}]$  cluster in which only the metal atoms and the bridging oxygen atoms (small circles) are shown. The manganese(IV) atoms are enhanced by the shadowing.

given by the envelope of the signals of the many transitions within the populated spin levels of the cluster at room temperature.

The last example we want to work out in detail is the one that has shown more similarities with bulk behavior, but we feel that, even in this case, we may still be a little far from that limit. There is a small family of clusters containing 12 manganese ions of general formula  $[\text{Mn}_{12}\text{O}_{12}(\text{carboxylato})_{16}]$ , referred to as  $\text{Mn}_{12}$  (Fig. 9). The carboxylates that have been investigated (38–41) so far are acetate and benzoate. The clusters are neutral. The external ring is formed by eight manganese(III) ions, with  $S = 2$ , and the internal tetrahedron is formed by four manganese(IV) ions, with  $S = 3/2$ . The valences are trapped, in the sense that there is no evidence of electron transfer between the two types of metal ions. The clusters are stable in solution, and other species have been obtained by standard redox procedures. It has been possible to substitute iron(III) ions for four of the manganese(III) ions (42). The magnetic properties of these materials are, however, less interesting than those of the parent  $\text{Mn}_{12}$  cluster.

The most intensively investigated compound of the series is the acetate, which has a tetragonal lattice and a crystallographically imposed  $S_4$  axis (38). The standard analysis of the magnetic properties strongly suggests a ground state with  $S = 10$  (40). This is justified if we assume that all the manganese(III) spins are up and all the manganese(IV) spins are down. This is perhaps an oversimplified view, and neutron diffraction experiments are under way to confirm it. The  $S = 10$  level seems to be well-separated from the excited levels.

Below 10 K, the measurements of the dynamic magnetic susceptibility, performed with the use of an oscillatory magnetic field, showed that the relaxation time of the magnetization is on the order of a few milliseconds (43). This is the behavior usually observed in superparamagnets; therefore,  $\text{Mn}_{12}$  seems to be a good candidate for investigation of the transition from simple paramagnetic to bulk behavior. All of the evidence, including specific heat data, is against a long-range magnetic order, that is, the observed phenomena are associated with the individual clusters and not with cooperativity effects among them.

The relaxation time of the magnetization rapidly increases with decreasing temperature. It has been experimentally found to be as long as 2 months at 2 K and to follow an exponential law like that of Eq. 3. The calculated energy barrier,  $E_A$ , is 61 K, and  $\nu_0$  is  $4.8 \times 10^6 \text{ s}^{-1}$ , much smaller than that usually found in superparamagnets. The magnetic anisotropy, responsible for

the high barrier to reorientation of the magnetization, is of the Ising type, that is, the easy axis is parallel to the  $S_4$  axis of the cluster and is determined by the sum of the contributions of the individual manganese(III) ions, which are in low-symmetry environments. At a microscopic level, this means that the ground  $S = 10$  level, which comprises 21 states characterized by quantum numbers  $M$  ranging from  $-10$  to  $10$ , is largely split in zero field in such a way that the  $M = \pm 10$  levels have the minimum energy. The other levels are found at energies  $E(M) = -M^2D$ , where  $D$ , the zero-field splitting parameter, is  $0.5 \text{ cm}^{-1}$ .

At low temperature, only the lowest levels are populated. To reverse its magnetization, a cluster must pass from the  $-10$  to the  $+10$  state by modulation mediated by phonons (44). However, it cannot do that directly because the transitions are allowed only between levels differing by  $\pm 1$  in  $M$ . Therefore, the spin component must pass from the  $-10$  state to  $-9$ , then to  $-8$ , up to  $M = 0$ , which is the highest in energy, and then descend down gradually to  $+10$ . This process is intrinsically slow and can be shown to follow an exponential law, which can be derived by extending the well-known Orbach mechanism of relaxation of the magnetization of paramagnets. Therefore, the "superparamagnetic" behavior of  $\text{Mn}_{12}$  is attributable to the fact that it has a large ground spin state and that the zero-field splitting of the levels is such that the two levels of maximum multiplicity are lowest in energy.

The most important factor is the presence, at low temperature, of large magnetic hysteresis, comparable to that observed in hard magnets (43). The hysteresis in the present case is not caused by the irreversibility of the domain wall motion, as in bulk magnets, but by the fact that a strong magnetic field destroys the barrier for the reversal of the magnetization and the relaxation becomes fast. In a field larger than 2 T, all the spins are parallel to the field. If the field is decreased, the spins are frozen in the aligned position until a negative field strong enough to melt the spin system is reached. Materials showing hysteresis effects are bistable and can be used to store information.

The  $\text{Mn}_{12}$  clusters therefore provide an example of magnetic bistability originated at the molecular level. Recently, a decanuclear manganese cluster was reported (45), made of four manganese(III) and six manganese(II) ions connected through  $\mu_4$  oxo bridges with an  $S = 12$  ground state. The anisotropy is again of the Ising type but is an order of magnitude smaller than that in  $\text{Mn}_{12}$ , and no superparamagnetic-like behavior has been observed down to 2 K.

## Conclusions

The field of molecular magnetism has been growing rapidly in the last few years, and the study of large molecular clusters of metal ions forms one of the areas that is expanding most rapidly. Very important progress has already been made, both in the synthetic aspects, where serendipity is not the only guide to development of new compounds, and in the understanding of the magnetic properties.

Much remains to be done, especially in the development of reliable and safe synthetic strategies, if real nanoscale molecular materials are to be obtained. The second important point that must be developed is that of theoretical models conceived especially for mesoscopic materials that are too complex to be treated as small clusters and yet do not afford the simplifications associated with translation symmetry of infinite lattices.

## REFERENCES AND NOTES

1. A. Caneschi *et al.*, *J. Am. Chem. Soc.* **110**, 2795 (1988).
2. R. D. McMichael, R. D. Shull, L. J. Swartzendruber, L. H. Bennett, *J. Magn. Magn. Mater.* **111**, 29 (1992).
3. R. F. Ziolo *et al.*, *Science* **257**, 219 (1992).
4. L. E. Brus *et al.*, *J. Mater. Res.* **4**, 704 (1989).
5. F. Palacio *et al.*, in *Physics and Chemistry of Finite Systems: From Clusters to Crystals*, P. Jena, Ed. (Kluwer Academic, Dordrecht, Netherlands, 1992).
6. S. Sarel *et al.*, *Inorg. Chem.* **28**, 4187 (1989).
7. M. P. J. van Staveren, H. B. Brom, L. J. de Jongh, *Phys. Rep.* **208**, 1 (1991).
8. P. C. E. Stamp, E. M. Chudnovsky, B. Barbara, *Int. J. Mod. Phys.* **6**, 1355 (1992).
9. A. J. Leggett, *Phys. Rev. B* **30**, 1208 (1984).
10. D. D. Awschalom, D. P. DiVincenzo, J. F. Smyth, *Science* **258**, 414 (1992).
11. J. Tejada *et al.*, *J. Appl. Phys.* **73**, 6709 (1993).
12. S. Mann, J. Webb, R. J. P. Williams, Eds., *Biomineralization: Chemical and Biochemical Perspectives* (VCH, New York, 1989).
13. F. C. Meldrum, B. R. Heywood, S. Mann, *Science* **257**, 522 (1992).
14. S. L. Heath and A. Powell, *Angew. Chem. Int. Ed. Engl.* **31**, 191 (1992).
15. G. C. Ford *et al.*, *Philos. Trans. R. Soc. London Ser. B* **304**, 551 (1984).
16. G. C. Papaefthymiou, *Phys. Rev. B* **46**, 10366 (1992).
17. S. C. Lee and R. H. Holm, *Angew. Chem. Int. Ed. Engl.* **29**, 840 (1989).
18. M. T. Pope, *Heteropoly and Isopoly Oxometalates* (Springer, New York, 1983).
19. A. Müller and M. T. Pope, Eds., *Polyoxometalates: From Platonic Solids to Anti-retroviral Activity* (Kluwer, Dordrecht, Netherlands, 1994).
20. A. Müller, *Nature* **352**, 115 (1991).
21. \_\_\_\_\_ and M. T. Pope, *Angew. Chem. Int. Ed. Engl.* **30**, 34 (1991).
22. A. Müller, J. Döring, M. I. Khan, V. Wittenben, *ibid.*, p. 210.
23. A. Müller and J. Döring, *ibid.* **27**, 1721 (1988).
24. \_\_\_\_\_, *Z. Anorg. Allg. Chem.* **595**, 251 (1991).
25. A. L. Barra, D. Gatteschi, A. Müller, J. Döring, *J. Am. Chem. Soc.* **114**, 8509 (1992).
26. J. Vannimenous and G. Toulouse, *J. Phys. C* **10**, 537 (1977).
27. D. Gatteschi and L. Pardi, *Gazz. Chim. Ital.* **123**, 231 (1993).
28. K. Wieghardt, K. Pohl, I. Jibril, G. Huttner, *Angew. Chem. Int. Ed. Engl.* **23**, 77 (1984).
29. K. L. Taft and S. J. Lippard, *J. Am. Chem. Soc.* **112**, 9629 (1990).
30. C. D. Delfs *et al.*, *Inorg. Chem.* **32**, 3099 (1993).
31. A. K. Powell *et al.*, in preparation.
32. K. L. Taft *et al.*, *J. Am. Chem. Soc.* **116**, 823 (1994).
33. L. Néel, *Ann. Geophys.* **5**, 99 (1949).
34. W. M. Reiff, in *Chemical Mössbauer Spectroscopy*, R. H. Herber, Ed. (Plenum, New York, 1984).
35. K. L. Taft *et al.*, *J. Am. Chem. Soc.* **115**, 11753 (1993).
36. K. L. Taft, G. C. Papaefthymiou, S. J. Lippard, *Science* **259**, 1302 (1993).
37. A. Bencini and D. Gatteschi, *Electron Paramagnetic Resonance of Exchange Coupled Systems* (Springer Verlag, Berlin, 1990).
38. T. Lis, *Acta Crystallogr. Sect. B* **36**, 2042 (1980).
39. P. D. W. Boyd *et al.*, *J. Am. Chem. Soc.* **110**, 8537 (1988).
40. A. Caneschi *et al.*, *ibid.* **113**, 5873 (1991).
41. R. Sessoli *et al.*, *ibid.* **115**, 1804 (1993).
42. A. R. Schake, *Chem. Commun.* **1992**, 181 (1992).
43. R. Sessoli, D. Gatteschi, A. Caneschi, M. Novak, *Nature* **365**, 141 (1993).
44. J. Villain, F. Hartman-Boutron, R. Sessoli, A. Rettori, *Europhys. Lett.*, in press.
45. D. P. Goldberg, A. Caneschi, S. J. Lippard, *J. Am. Chem. Soc.* **115**, 9299 (1993).
46. We are indebted to A. K. Powell, S. J. Lippard, A. Müller, and K. Wieghardt. The financial support of the Human Capital and Mobility Programme of the Commission of the European Community (grant ERBCHRXCT920080) is also acknowledged.